International Journal of Food Microbiology 279 (2018) 33–42

Contents lists available at ScienceDirect

International Journal of Food Microbiology

journal homepage: www.elsevier.com/locate/ijfoodmicro

Bactericidal and antibiofilm activity of bactenecin-derivative peptides against the food-pathogen *Listeria monocytogenes*: New perspectives for food processing industry

Gianna Palmieri[a,b,*,1], Marco Balestrieri[a,b,1], Federico Capuano[c], Yolande T.R. Proroga[c], Francesco Pomilio[d], Patrizia Centorame[d], Alessia Riccio[a], Raffaele Marrone[e], Aniello Anastasio[e]

[a] Institute of Biosciences and BioResources (IBBR)-UOS Na, National Research Council (CNR-IBBR), Via Pietro Castellino 111, 80131 Naples, Italy
[b] Materias S.r.l., Corso N. Protopisani n. 50, 80146 Naples, Italy
[c] Department of Food Microbiology, Istituto Zooprofilattico Sperimentale del Mezzogiorno, via della salute, 2, 80055 Portici, Italy
[d] National reference laboratory for Listeria monocytogenes, Istituto Zooprofilattico Sperimentale dell'Abruzzo e del Molise, Via Campo Boario 1, 64100 Teramo, Italy
[e] Department of Veterinary Medicine and Animal Production, University of Naples Federico II, Via Federico Delpino 1, 80137 Naples, Italy

ARTICLE INFO

Keywords:
Antimicrobial/antibiofilm peptide
Innate defense regulator peptide
Foodborne pathogens
Listeria monocytogenes
Food bio-preservatives

ABSTRACT

Antimicrobial peptides have received great attention for their potential benefits to extend the shelf-life of food-products. Innate defense regulator peptide-1018 (IDR-1018) represents a promising candidate for such applications, due to its broad-spectrum antimicrobial activity, although food-isolated pathogens have been poorly investigated. Herein, we describe the design and the structural-functional characterization of a new 1018-derivative peptide named 1018-K6, in which the alanine in position 6 was replaced with a lysine. Spectroscopic analysis revealed a noticeable switch from β-sheet to helical conformations of 1018-K6 respect to IDR-1018, with a faster folding kinetic and increased structural stability. Moreover, 1018-K6 evidenced a significant antibiofilm/bactericidal efficiency specifically against *Listeria monocytogenes* isolates from food-products and food-processing environments, belonging to serotype 4b involved in the majority of human-listeriosis cases, with EC_{50} values two- five-fold lower than those measured for IDR-1018. Therefore, a single amino-acid substitution in IDR-1018 sequence produced severe changes in peptide conformation and antimicrobial performances.

1. Introduction

Listeria monocytogenes is a ubiquitous, facultative intracellular bacterium, which is potentially pathogenic for humans. Through the ingestion of contaminated food products, this bacterium can cause serious infections that are life-threatening (*e.g.* meningitis, perinatal and fetal infections) (Hernandez-Milian and Payeras-Cifre, 2014; Jensen et al., 2016) that can be life-threatening in at-risk populations, such as immune-compromised individuals and pregnant women. Indeed, unlike many other foodborne bacteria, *Listeria* can tolerate salty environments, survive and multiply at cold temperatures (between 2 °C and 4 °C) and grow in biofilms (Carpentier and Cerf, 2011; Stewart, 2015). In the food industry, biofilms cause serious health and engineering problems, as pathogenic microflora grown on food surfaces and in processing environments can produce post-processing contamination and cross-contamination from raw sources.

In the last two decades, the incidence of listeriosis epidemics has significantly increased (Jensen et al., 2016), with a case fatality rate around 20% and epidemiological studies strongly support the idea of a virulence variability of L. *monocytogenes* strains (Hernandez-Milian and Payeras-Cifre, 2014; Jensen et al., 2016). Currently, among a large number of serotypes so far identified, strains belonging to serotypes 1/2a, 1/2b, 1/2c, and 4b are responsible for 98% of listeriosis cases in humans, being 4b the most frequently associated with outbreaks (Ayaz and Erol, 2010; Hernandez-Milian and Payeras-Cifre, 2014; Orsi et al., 2011) and 1/2c one of the most resistant to antibiotics (Ayaz and Erol, 2010).

Therefore, taking into account the strong impact of foodborne diseases on human health and the growing consumer's attention on the use of chemical agents, natural substances such as antimicrobial peptides (AMP), assumed relevant interest for their great potential to be used as bio-preservatives. During the last few years, the widespread appearance of naturally occurring AMPs has been established in humans and other mammalian organisms. AMPs (De Smet and Contreras, 2005) are

* Corresponding author at: Via Pietro Castellino 111, 80131 Napoli, Italy.
E-mail address: gianna.palmieri@ibbr.cnr.it (G. Palmieri).
[1] These authors contributed equally to this work.

https://doi.org/10.1016/j.ijfoodmicro.2018.04.039
Received 22 December 2017; Received in revised form 23 April 2018; Accepted 24 April 2018
Available online 27 April 2018
0168-1605/ Published by Elsevier B.V.

essential components of innate immunity, contributing to the first line of defense against infections (Bals, 2000; Henzler Wildman et al., 2003). The effectiveness and selectivity of AMPs are related to their physicochemical properties including the amphipathic nature, net charge, hydrophobicity, and conformational flexibility (Falcigno et al., 2016; Palmieri et al., 2016; Zelezetsky and Tossi, 2006). This latter has been extensively investigated by Circular dichroism (CD) spectroscopy, which can provide useful information about the conformations and the extent of the structural changes of peptides. CD relies on the differential absorption of left and right circularly polarized radiation by chromophores. Peptides possess a number of chromophores, which show intrinsic chirality and can give rise to CD signals. Therefore, in the far UV region, corresponding to peptide bond absorption, CD spectra can be analyzed to give a picture of the conformational status of a peptide and the content of regular secondary structural features such as alpha-helix and beta-sheet.

AMPs can permeabilize the membranes and form cytotoxic pores but they can also inhibit cell wall, nucleic acid, and protein biosynthesis. AMPs family comprises peptides showing also antibiofilm activity, ABPs (antibiofilm peptides), which usually are short and amphipathic with a high number of basic residues (R or K) and at least 50% of hydrophobic amino-acids (Amer et al., 2010; de la Fuente-Núñez et al., 2012; de la Fuente-Núñez et al., 2014a; Overhage et al., 2008; Pompilio et al., 2011). These compounds exhibit specific activity against bacterial biofilms at concentrations frequently below their minimal inhibitory concentration (MIC) for planktonic cells (Amer et al., 2010; de la Fuente-Núñez et al., 2012, 2014a; Overhage et al., 2008; Pompilio et al., 2011) and no correlation between antibiofilm and antiplanktonic cell activity has been often observed (Overhage et al., 2008).

Recently, Hancock and co-authors have developed a peptide, called innate defense regulator (IDR)-1018, displaying a broad-spectrum antibiofilm activity (de la Fuente-Núñez et al., 2012, 2014a; Reffuveille et al., 2014). IDR-1018 is a natural 12-amino-acid peptide (VRLIVAVRIWRR-NH_2) derivative of bactenecin, the bovine host-defense peptide (HDP), which belongs to the cathelicidins family. Several studies, carried out over recent years, attribute relevant functions to this peptide and specifically: *i*) antibiofilm activity towards a broad spectrum of pathogenic bacteria (de la Fuente-Núñez et al., 2012, 2014a; Reffuveille et al., 2014); *ii*) induction of lymphocytes and regulation of the cytokine production (Pena et al., 2013; Wieczorek et al., 2010); *iii*) reduction of tissue infections (Wieczorek et al., 2010). Antimicrobial activity of IDR-1018 was demonstrated against a large panel of Gram-negative bacteria and the Gram-positive *Staphylococcus* strains (*Staphylococcus aureus*, *Staphylococcus epidermidis*) with MIC values ranging from 5 to 260 μg/ml, (de la Fuente-Núñez et al., 2014a; Reffuveille et al., 2014; Wieczorek et al., 2010) but it was never tested towards *Listeria* species.

The purpose of our study was to identify new anti-*Listeria* compounds able to counteract efficiently the growth of this foodborne microorganism and displaying high structural-functional stability in a wide range of environments associated with contaminated food-products and food-processing devices. Therefore, here we describe the design and the characterization of a novel 1018-derivative peptide, which reveals an improvement in the conformational stability and bactericidal/antibiofilm activity in comparison with the parent IDR-1018, specifically against L. *monocytogenes* strains isolated from food and environmental samples collected from dairy product and canned food industries. In addition, our data demonstrated that a single residue variation in IDR-1018, produced a molecule with increased propensities for helical structuring, which appeared to be a key parameter in modulating antimicrobial activity towards L. *monocytogenes*, even though observed in membrane-mimetic models such as micellar solutions of sodium dodecyl sulfate (SDS)·This well-known ionic detergent, consisting of a hydrophobic 12-carbon chain and a polar sulfate head group, has amphiphilic properties that allow to form micelles, which are widely employed to mimic the lipid bilayer systems in structural studies of bacterial membrane-targeting peptides (Parker and Song, 1992).

2. Materials and methods

2.1. Materials

Peptides were purchased from SynPeptide Co., LTD (Shanghai, China). DMSO (Dimethyl sulfoxide), SDS (Sodium Dodecyl Sulfate) and other chemicals, when not specified, were from Sigma-Aldrich (St. Louis, Missouri, USA).

2.2. In silico selection of AMPs

The designing strategy to identify new potential AMPs was based on antimicrobial activity and structural stability predictions performed with computational tools at the Antimicrobial Peptide Database (http://aps.unmc.edu/AP/) and the ProtParam (https://web.expasy.org/protparam/) web sites. Among the different parameters computed, the Boman index (Boman, 2003) prediction tool calculates the protein-binding potential and it is generally adopted for the *in silico* evaluation of the antimicrobial functions. The Boman index is obtained by the sum of the free energies of the respective amino-acid side chains for transfer from cyclohexane to water taken from Radzeka and Wolfenden (Radzicka and Wolfenden, 1988) and divided by the total number of peptide residues.

2.3. Sampling, isolation and characterization of Listeria strains used for bactericidal activity assay

During the study period (2015–2016), 150 samples from seafood products and food-processing environments (dairy product and canned food industries), were collected from markets, in southern Italy, in the context of official controls. The isolation of five *Listeria monocytogenes* strains was carried out according to the ISO 11290-1 (ISO 11290-1:1996/Amd 1, 2004). These strains (LM1-LM5) were characterized by serotyping (FDA/CFSAN, 2002, Bacteriological analytical manual (BAM); Gilot et al., 1996) and Pulsed Field Gel Electrophoresis (PFGE) analysis according to PulseNet protocol (PulseNet-International, 2013), involving the restriction enzymes *Asc*I and *Apa*I using sera for somatic (O) and flagellar (H) antigens (Denkan Seiken Co. Ltd., Tokyo, Japan) (Table S1).

2.4. Circular dichroism spectroscopy

Circular Dichroism (CD) analysis was performed by Jasco J-810 spectropolarimeter equipped with a thermostated cuvette compartment. The samples (0.1 g/L) were loaded into a quartz cuvette of 0.1 cm path length (Hellma Analytics) and the spectra were recorded at 15 °C or 90 °C, in the 190 nm–250 nm range at a scan speed of 20 nm/min, by averaging 5 scans and in presence of 3 or 10 mM SDS. The effect of pH on the secondary structure of the peptides was evaluated by dissolving the samples in different buffer solutions at concentration of 10 mM: potassium chloride-HCl, pH 1.0; glycine-HCl, pH 2.0; sodium acetate, pH 4.0 and 6.0; Tris-HCl, pH 8.0; glycine-NaOH, pH 10.0; sodium bicarbonate-NaOH, pH 11.0. Then, after 1 h incubation at 25 °C, SDS (10 mM final concentration) was added to each sample, which was incubated for further 24 h at 25 °C and analyzed by CD spectroscopy. The mean residue ellipticity ([θ], deg. cm^2 $dmol^{-1}$) was obtained by the equation $[\theta] = 100\,\theta/cnl$, where θ is the ellipticity (mdeg), c is the peptide concentration (mM), n is the number of residues, and l is the path length (cm).

The folding kinetic measurements of the peptides were carried out by CD after addition of SDS (10 mM final concentration) to each sample (0.1 g/L in sodium acetate buffer 10 mM, pH 6.0), over 24 h incubations. CD spectra were recorded in the 195 nm–250 nm range at 25 °C. In all analyses, the percentage of secondary structure was estimated by

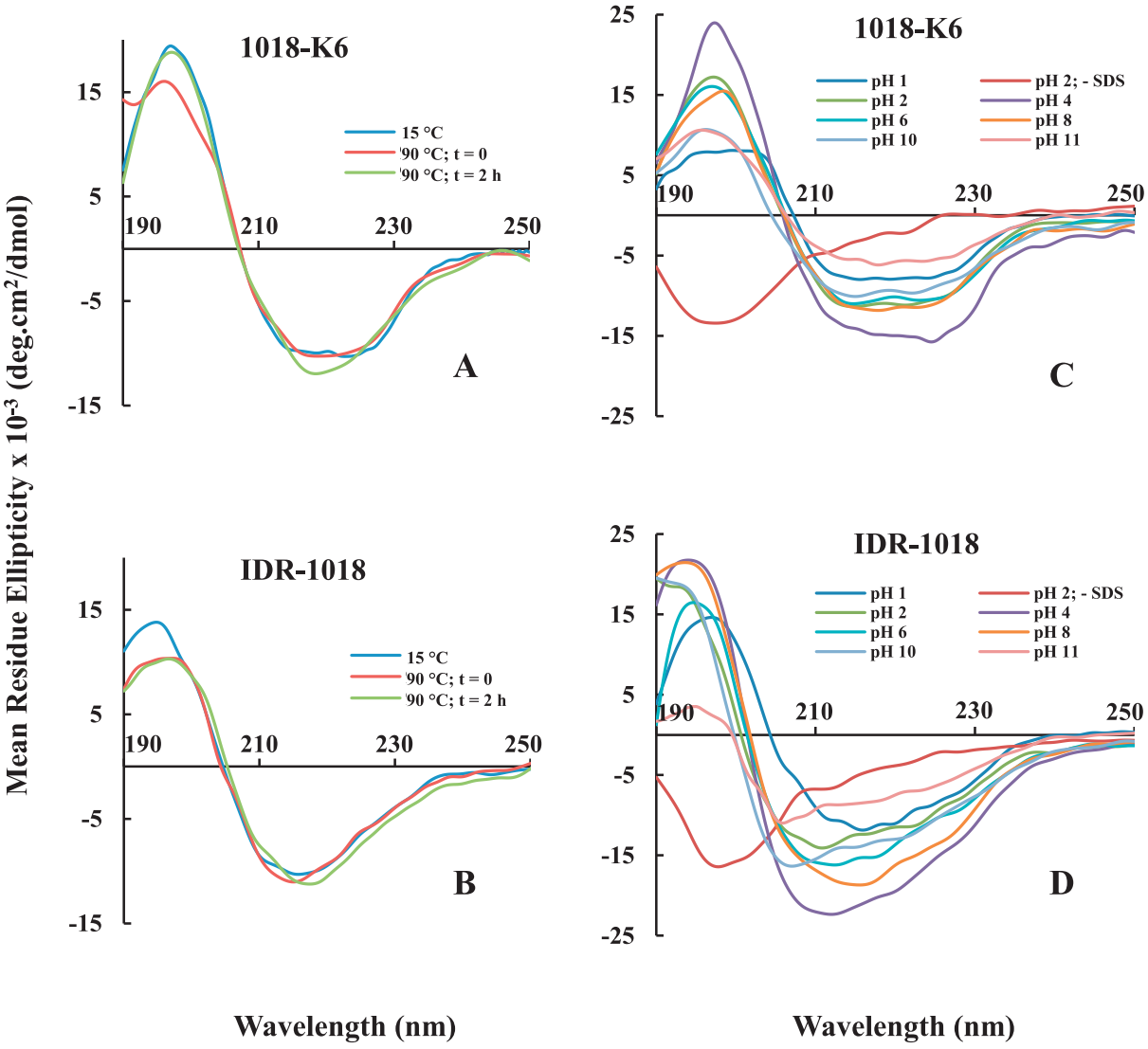

Fig. 1. Effect of pH and temperature on the secondary structure of 1018-K6 and IDR-1018 peptides. CD spectra were obtained by dissolving each peptide at 0.1 g/L in sodium acetate buffer 10 mM, pH 6.0 in the presence of 10 mM SDS. The spectra of 1018-K6 (A) and IDR-1018 (B) were recorded, in the 190 nm–250 nm range at 15 °C or before and after incubation for 2 h at 90 °C.
CD spectra of 1018-K6 (C) and IDR-1018 (D) obtained by incubating each peptide at 0.1 g/L in different buffers (see Materials and Methods section), for 24 h at 25 °C and in the presence of 10 mM SDS. The spectra of peptide samples incubated for 24 h without SDS in the buffer at pH 2.0 were also showed.

the DICHROWEB site (Lobley et al., 2002; Whitmore and Wallace, 2004, 2008), using three different algorithms (SELCON3, CONTIN-LL and CDSSTR) (Sreerama and Woody, 2000; Van Stokkum et al., 1990) and the protein dataset from Abdul-Gader et al., 2011.

2.5. Fluorescence measurements

The peptide folding kinetic measurements were also performed by fluorescence spectroscopy at 25 °C using a Jasco FP-8200 spectrofluorometer at pH 6.0 (10 mM sodium acetate buffer), following the addition of SDS (10 mM final concentration) to each peptide sample (0.1 g/L). Fluorescence emission from tryptophan residue was detected in the 300 nm–400 nm wavelength range, using excitation at 280 nm and setting the excitation and emission slit widths of 5 nm. As described above, the fluorescent signals were recorded over 24 h incubation.

2.6. Bactericidal activity assays

The antimicrobial efficacy of the two bactenecin-derived peptides was determined against *S. aureus* (ATCC 25923), *L. monocytogenes* (NCTC 1911 and five food-isolated strains described above) and *S.* Typhimurium (ATCC 13311) bacteria, which allowed the evaluation of the minimal bactericidal concentration (MBC) and the half-maximal effective concentration (EC_{50}). The MBC, corresponding to the lowest peptide concentration at which no growth was observed on agar plates, was measured as reported below. The EC_{50} values (peptide concentration at which 50% of the maximal number of colonies was observed) of the two peptides were determined with broth microdilution assay as described by Palmieri et al., 2016. Standard deviations of triplicate incubations for each plate and EC_{50} evaluation were determined using GraphPad Prism version 6.00 (Graph-Pad Software, La Jolla California USA, www.graphpad.com).

2.6.1. Bacterial strains

A concentration of 10^3 CFU of the selected bacteria strains (*L. monocytogenes*, *S.* Typhimurium, *S. aureus*) was inoculated in 10 ml of growth broths (*L. monocytogenes* Half Fraser, Biorad- Italia; *S.* Typhimurium and *S. aureus* BPW, Biomerieux- Italia). Stock solutions

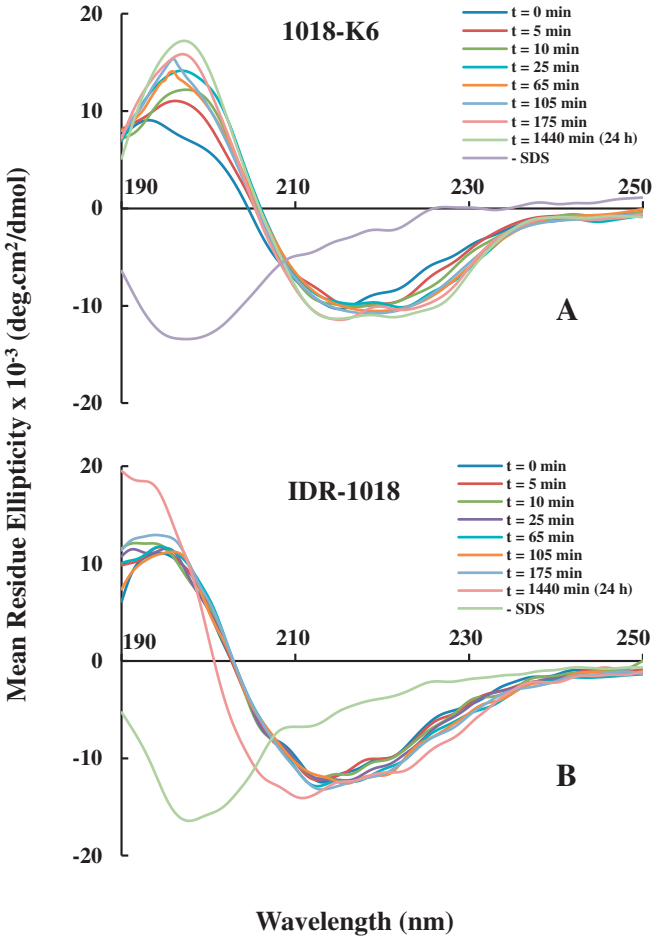

Fig. 2. Conformational changes of 1018-K6 and IDR-1018 as a function of time. CD spectra of 1018-K6 (A) and IDR-1018 (B) at a concentration of 0.1 g/L in sodium acetate buffer 10 mM, pH 6.0, were recorded in the 195 nm–250 nm range at 25 °C, after addition of 10 mM SDS over 24 h incubations. For clearness, only the spectra obtained at the indicated times were reported.

(5 mM) of the two peptides dissolved in DMSO were used for the preparation of serial dilutions in broths, and then inoculated with the bacteria and incubated for 6 h at 37 °C. In this way, 50 µl of each bacterial suspension were spread onto two different culture plate, a blood agar plate and a further culture plate appropriately selected based on the bacteria strain (*L. monocytogenes*, ALOA – Biolife Italia; *S.* Typhimurium, *Salmonella* Chromogenic agar - Oxoid UK; *S. aureus*, Rabbit Plasma Fibrinogen agar – Biolife Italia) and were incubated for 20–48 h at 37 °C. Each dilution series included control plates with only bacteria and DMSO without peptide. In all the experimental conditions explored, the plate counting method was used to estimate the bactericidal activity of the peptides. Specifically, the number of colonies grown on agar plates in the absence or presence of the different dilutions of peptides were counted and compared. Standard deviations of triplicate incubations for each plate were determined by using Microsoft®Excel 2000/XLSTAT©-Pro.

2.7. Antibiofilm activity assay

L. monocytogenes cultures (ATCC 7644 and EURL12MOB098LM isolated from dairy products) were prepared to inoculate BHI broth (Brain Heart Infusion, Sigma-Aldrich, St. Louis, Missouri, USA) at 37 °C up to a logarithmic phase of growth. After the incubation, 10 ml of bacterial suspension was centrifuged, the cell pellet was washed in PBS pH 7.3 (Thermo Fisher Scientific Inc., Waltham, Massachusetts, USA) and diluted in BHI broth to reach the concentration of about 10^3 CFU/ml of the standardized inoculum.

The biofilm formation assays were conducted using as target surface the stainless steel Aisi 304 coupons (diameter 14.5 mm) (SS) used as food contact surfaces in the food industry. The SS were placed into the 24 well tissue culture plates (Falcon, Thermo Fisher Scientific Inc.,Waltham, Massachusetts, USA), with flat bottom and lid. Before use, the SS were immersed in 10% acetone and left under gentle shaking (shaker Stuart, Bibby Scientific Limited, Staffordshire, UK) at room temperature. After washing in sterile ultrapure water (IZSAM), the SS were incubated in ethanol (≥99.8%) for 10 min under gentle shaking and then washed in sterile ultrapure water, dried, packaged and sterilized at 121 °C, 1 atm for 15 min. In each experiment set, 600 µl of the standardized inoculum in the presence or absence of each peptide at different concentrations (12.5, 25, 50 µM), was added to 24 well tissue culture plates containing SS previously treated. BHI broth was used as negative control and the plates were incubated at 37 °C for 72 h in the static condition. Cell counting of L. *monocytogenes*, in agreement to ISO 11290-2:98 (ISO 11290-2: 1998/Amd 1, 2004) method was performed to assess the concentration and purity of the standardized inoculum. After incubation, SS were washed three times with PBS and placed in a new plate to dry (60 °C for 1 h). At the end of the fixing phase, 1 ml of 0.2% Crystal Violet (Panreac Quimica SAU, Barcelona, Spain) in 95% ethanol was added to each well to stain the SS. After gently shaking for 15 min, the SS were washed three times with sterile water and then transferred into a new plate to dry at 37 °C. The quantitative analysis of biofilm production was performed by adding 1 ml of 33% acetic acid to destain the SS and 200 µl of each solution was transferred to a microtiter plate to measure the level (OD_{492}) of the crystal violet.

All antibiofilm assays were performed in triplicate in three independent sets of experiments for each peptide. OD_{492} values were compared through non-parametric analysis of variance (Kruskal-Wallis test), followed by multiple comparisons using the Dunn test pairs (with Bonferroni correction) ($p < 0.05$). Statistical analyses were performed using Microsoft®Excel 2000/XLSTAT©-Pro.

2.8. SEM of L. monocytogenes biofilm

Three-dimensional architecture of biofilm developed on SS has been studied by using the scanning electron microscopy (SEM). The SS were extensively washed with sterile PBS to remove planktonic cells and fixed in a new plate with 1 ml of Karnovsky's fixative (final mixture 5% glutaraldehyde, 4% paraformaldehyde in 0.064 M buffer) (Electronic Microscopy Science, Hatfield, PA, USA) for 1 h at 4 °C. Then, samples were washed in 0.1 M sodium cacodylate buffer (Electronic Microscopy Science, Hatfield, PA, USA) pH 7.4 and the fixed cells were dehydrated in a series of aqueous acetone solutions (as a sequence of 25%, 50%, 75%, 95% and 100% concentration). Samples were glued onto polished aluminum stubs (Electronic Microscopy Science, Hatfield, PA, USA) and coated uniformly under vacuum with a layer of about 20 nm thickness of gold with a K950 High Vacuum Turbo Evaporator and K 350 Attachment (Emitech Ltd., Ashford, UK). Coated samples were examined under a JEOL 6700 FEG–field emission Scanning Electron Microscope (SEM Jeol, city and state) at 1000 to 5000 magnifications. Several images were randomly evaluated in each sample, recorded and archived as an electronic image, only the most representative was shown.

2.9. Peptide stability in mozzarella cheese brine

The peptide stability in mozzarella cheese brine was examined by reverse-phase (RP) High-Performance Liquid Chromatography (HPLC) (Shimadzu Prominence, Modular HPLC - Shimadzu Italia S.r.l.) on a µBondapak C18 column 3.9 × 300 mm (Waters SpA, Milano - Italia), eluted by a linear gradient of 5–95% acetonitrile in water with 0.1%

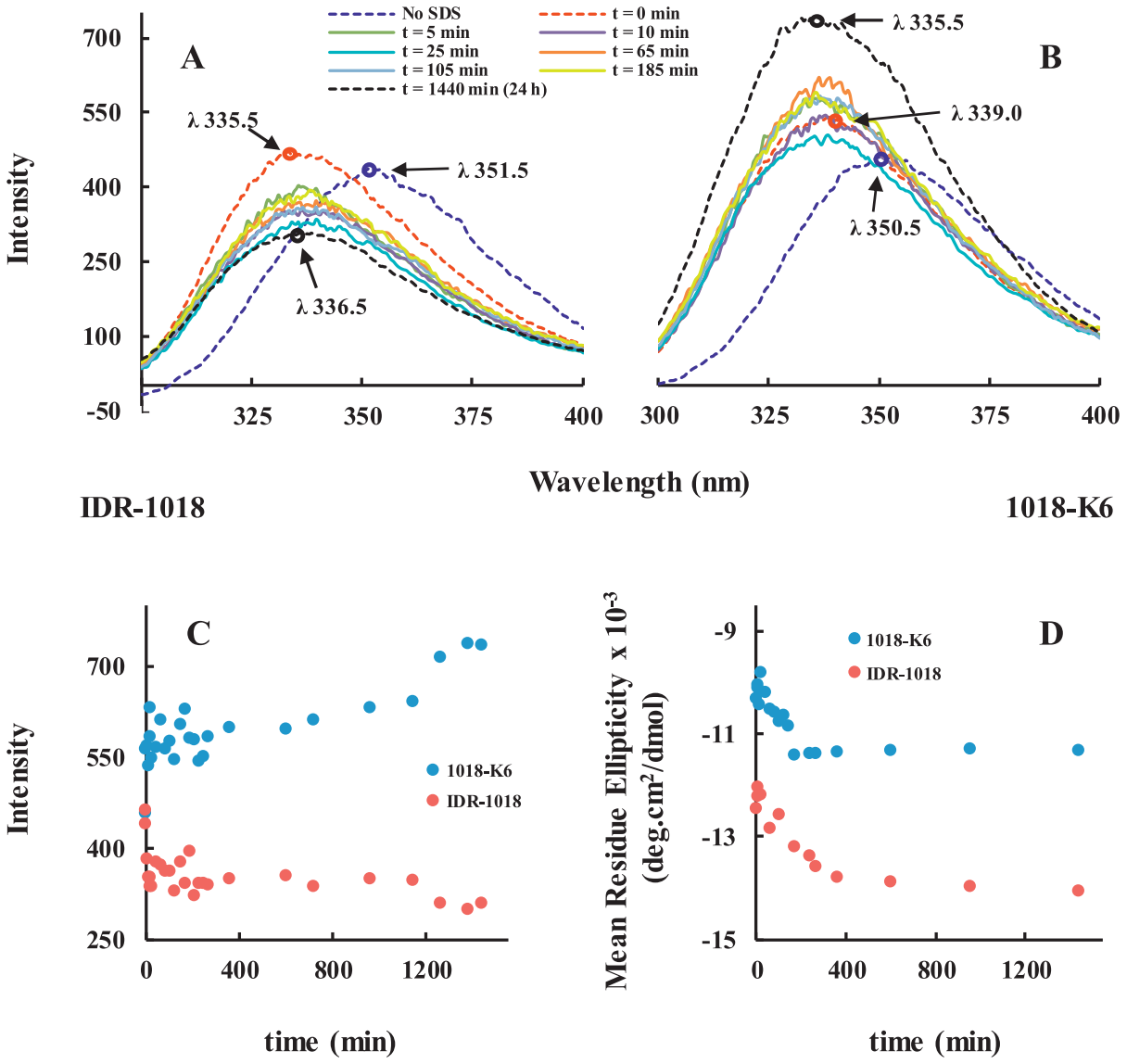

Fig. 3. Peptide Folding monitored by Fluorescence and CD spectroscopy. Peptide fluorescence spectra were recorded from 300 to 400 nm with the spectral widths of excitation and emission slits set at 5 nm, using excitation wavelength of 280 nm. The fluorescence signals (A, B) were monitored over 24 h after the addition of SDS 10 mM to each peptide (0.1 g/L) dissolved in sodium acetate buffer 10 mM, pH 6.0 at 25 °C. Time trend of the maximum fluorescence intensity values, measured for each peptide, over 24 h incubation after the addition of SDS (10 mM final concentration) (C); Time trend of the mean residue Ellipticity values corresponding to the minimum wavelength over 24 h incubation after the addition of SDS to each peptide (0.1 g/L) dissolved in sodium acetate buffer 10 mM, pH 6.0 at 25 °C (D).

TFA at a flow rate of 1 ml/min. Each peptide was incubated in different mozzarella cheese brines for 24 h at 4 °C and then loaded onto the RP column. Control samples treated under the same conditions in the absence of peptides were run in parallel (Palmieri et al., 2016).

3. Results and discussion

3.1. Design and in-silico prediction of physicochemical properties of bactenecin-derivative peptides

Thus far, several strategies have been used for the rational design of AMP with improved activity and stability. Even though the structural requirements that play a crucial role in controlling microbial colonization or density have not been completely elucidated, it is becoming clear that the mechanisms by which AMPs perform their functions are governed by a specific set of measurable physicochemical properties resulting from the amino-acid sequence. Moreover, all these parameters can strongly affect the structural stability of AMPs under specific environmental conditions.

Herein, by using a simple *in silico* strategy starting from the peptide IDR-1018 (VRLIVAVRIWRR-NH2), a well-known antibiofilm compound, two molecules were designed *ex-novo* and predicted to be highly stable and antimicrobic: *i*) the 12-mer peptide, 1018-K6 reproducing the IDR-1018 sequence with the replacement of the alanine in position 6 with a lysine (A6 → K6 mutation); *ii*) the 12-mer peptide, 1018-K10, with W10 → K10 mutation. In our approach, all the amino-acidic positions in the IDR-1018 sequence were sequentially mutated introducing a K residue to further increase the positive charge, which is one of the most critical factors for improving the potential interaction of antimicrobial agents with the outer membrane of bacteria. Hence, the resulting peptides were *in silico* analyzed by the computational tools at the Antimicrobial Peptide Database website (Wang et al., 2016) and the ProtParam tools at the ExPASy Bioinformatics Resource Portal. The evaluation of the Boman index (Radzicka and Wolfenden, 1988), which is a measure of the peptide affinity to proteins and of the ability to establish biological interactions, was first used to identify which

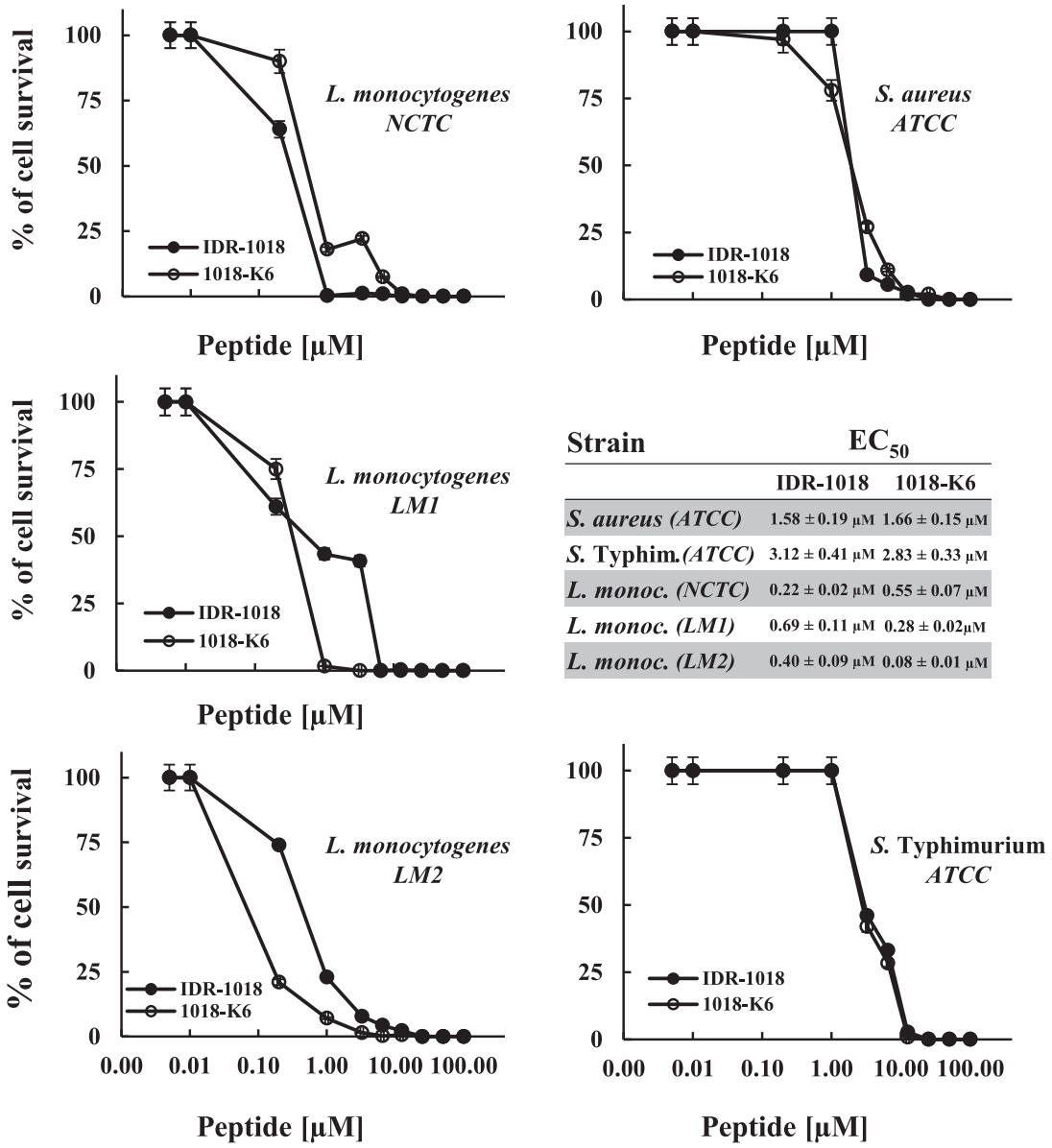

Strain	EC_{50}	
	IDR-1018	1018-K6
S. aureus (ATCC)	1.58 ± 0.19 μM	1.66 ± 0.15 μM
S. Typhim.*(ATCC)*	3.12 ± 0.41 μM	2.83 ± 0.33 μM
L. monoc. (NCTC)	0.22 ± 0.02 μM	0.55 ± 0.07 μM
L. monoc. (LM1)	0.69 ± 0.11 μM	0.28 ± 0.02μM
L. monoc. (LM2)	0.40 ± 0.09 μM	0.08 ± 0.01 μM

Fig. 4. Bactericidal activity of IDR-1018 and 1018-K6 on different foodborne bacteria. The dose-dependent killing curves were determined by enumeration of the surviving colony forming units (CFU) on plates, seeded with the indicated pathogen incubated with the different peptide concentrations. Data were expressed as percent of CFU survival, respect to the colony counted in the control plates. The EC_{50} values of the two peptides measured for the indicated bacteria were also reported. Standard deviations of triplicate incubations for each plate and EC50 evaluation were determined using GraphPad Prism version 6.00.

mutation produced a reduction in the potential antimicrobial peptide activity (Table S2). As expected by considering the total net charge, the replacements of R residues into K, dramatically decreased the Boman index values respect to those determined for the remaining peptides under investigation, (ranging from 3.0 to 3.3 Kcal/mol) in which the substitution of all the other amino acids into K, generated an extra positive charge.

The assessment of further physicochemical parameters (Table S2) suggested that both 1018-K6 and 1018-K10 peptides were good candidates to study the structural and functional properties potentially useful for biotechnological applications in food industry. In detail, apart from the computed Boman index data, computational investigations predicted the highest values of aliphatic and GRAVY index (Table S2) for 1018-K6 and 1018-K10, which positively correlate with the structural stability and thermal resistance (Wang et al., 2016). This evidence was also in agreement with the instability index (Guruprasad et al., 1990) especially in the case of 1018-K6, possibly figuring a greater conformational stability *in vitro* of this peptide (Table S2).

3.2. Structural characterization of 1018-K6 in comparison with IDR-1018

As mentioned before, the stability and function of AMPs strongly depend on their structure, hence it is important to get as much information as possible on novel peptides when designing, with the aim of expanding their possible industrial applications (Palmieri et al., 2016; Zelezetsky and Tossi, 2006).

Firstly, a study on IDR-1018 and the two derivatives 1018-K6 and 1018-K10, resulting from the computational analysis, was carried out by CD and steady-state fluorescence spectroscopy to provide a picture of the structure and conformational changes of these molecules in relation to a range of environmental conditions. Preliminary results (data not shown) predicted that the peptide 1018-K6 was the best molecular model to continue our analysis and it was selected for further investigations in comparison with IDR-1018. This choice was also

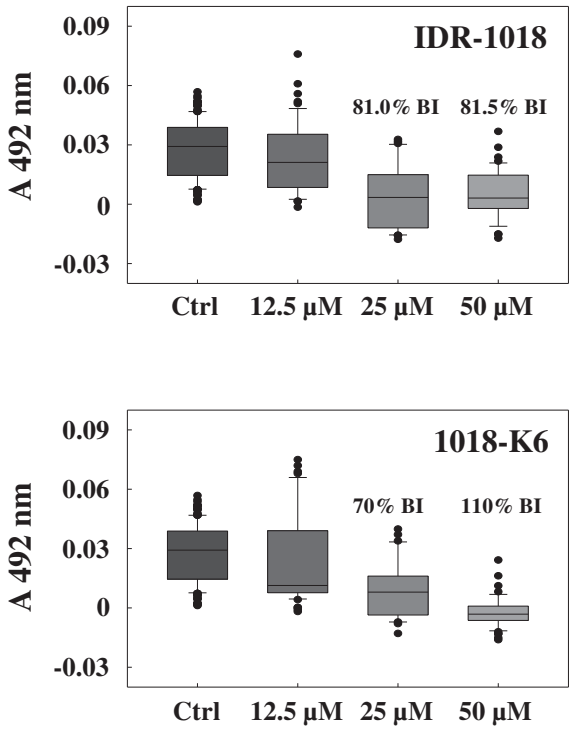

Fig. 5. Dose-dependent antibiofilm effect of IDR-1018 and 1018-K6 on L. *monocytogenes*.

L. monocytogenes was grown under biofilm conditions in the absence (Ctrl) or presence of 12.5, 25 and 50 µM of each peptide on SS. After growth at 37 °C for 72 h, biofilm formation was assessed by CV staining and quantified following the Absorbance at 492 nm (A_{492}). Box plots showed the distributions of A_{492} measurements upon peptides treatments across the sample groups. Statistical analysis was performed on triplicate sets of experiments, significance (p-value < 0.001) was confirmed by multiple comparisons using the Dunn test pairs (with Bonferroni correction). Pairwise comparisons showed significant differences between control and samples with 25 µM or 50 µM for each peptide. No significant differences were evidenced by pairwise comparisons when each peptide was evaluated at 12.5 µM concentration. Median (horizontal line in the box), 25th and 75th percentiles (edges of box), maximum and minimum values (whiskers) were shown in the box plots. Quantitative biofilm Inhibitions (BI %) determined for each peptide respect to the Ctrl were also reported. OD_{492} values were compared through non-parametric analysis of variance (Kruskal-Wallis test), followed by multiple comparisons using the Dunn test pairs (with Bonferroni correction) ($p < 0.05$).

reinforced by the absence of tryptophan residues in 1018-K10 sequence, making it impossible to perform fluorescence measures. Therefore, to evaluate the secondary structure of the two peptides in a condition mimicking the cell membranes, CD spectra were recorded in 3 or 10 mM SDS micelles (CD data at 3 mM SDS were only registered for 1018-K6 due to the limited solubility of IDR-1018 under this condition, Table S3) and at 15 °C or 90 °C temperatures. Intriguingly, while IDR-1018 assumed a predominant β-sheet structure, as revealed by the typical signals in CD spectra (Wieczorek et al., 2010), conversely the two negative bands at 215 nm and 222 nm clearly evidenced that the main conformational status of 1018-K6 involved α-helix structures (Fig. 1). In addition, after incubation for 2 h at 90 °C, the two peptides conserved their conformation, (Fig. 1A, B) suggesting a remarkable thermostability as predicted by *in silico* analysis. Therefore, a single point mutation (A → K) in the IDR-1018 sequence was able to trigger a large conformational change, increasing the propensity for helical structuring, which can significantly affect the antimicrobial performances. The reliability of the predicted structural features was improved by using three different algorithms (see Methods sections) provided by the Dichroweb on-line server (Lobley et al., 2002; Whitmore and Wallace, 2008, 2004) and choosing as reference protein dataset the SMP180, which includes a high number of soluble and membrane protein spectra (Abdul-Gader et al., 2011). Results confirmed that in SDS micellar solution (10 mM), 1018-K6 displayed a β-sheet content generally lower than that observed for IDR-1018 and a higher level of α-helix fold (Table S3), which was increased respect to that resulting from measurements at 3 mM SDS. These findings indicate that 1018-K6 can be included into the important class of α-helical AMPs (Zelezetsky and Tossi, 2006), having a suitable propensity for helix formation only at the membrane surface and being present as unstructured, random coil form in buffer solutions. This AMP cluster frequently tend to be bacteria selective and their behavior in simple model systems, such as SDS micelle, correlates well to the bacterial membrane permeabilization and killing activities (Zelezetsky and Tossi, 2006).

3.2.1. pH stability

In order to assess the structural stability in a wide range of pHs, peptide samples were incubated for 24 h in different buffers (pH range 1.0–11.0) in the presence of SDS and then analyzed by CD (Fig. 1). In absence of SDS, a broad negative band at 198 nm typically of random coil structures was observed in all CD spectra, while 1018-K6 and IDR-1018 were mainly in the α-helix or β-sheet conformations, respectively, in all conditions investigated (Fig. 1C, D). Indeed, structural perturbations over the entire pH interval were more evidenced for IDR-1018, respect to 1018-K6, which appeared to better maintain its structural integrity over the 24 h incubations. Overall, the percentage of secondary structure content was evaluated using three algorithms (data not shown) and results measured at extreme pHs (pH 1.0 and 11.0) were reported in Fig. S1, revealing a higher conformational stability at pH 1.0 respect pH 11.0 of IDR-1018, while the opposite was observed for 1018-K6 (Fig. S1). In light of this, a suitable combination of the two peptides could be useful to guarantee the structural integrity over a broader pH range, as a prerequisite for large applications in food industry.

Moreover, in order to preliminarily explore the behavior of the two peptides in conditions associated with the food supply chain of the dairy products whose complexity can strongly affect their antibacterial activity, mozzarella cheese brining was selected to examine the peptide stability. Indeed, mozzarella is one of the most well know soft cheese in Italy and represents a relevant component of the Mediterranean diet. However, mozzarella-like other soft cheeses, are likely to become contaminated with microbial pathogens because they have a relatively high moisture content, which creates a more hospitable environment for the bacterial growth. The ability of L. *monocytogenes* to survive and grow at high salt concentrations and low pH and temperatures, which are conditions found in mozzarella brines, prompted us to choose these environments in our analyses. As shown in Fig. S2, IDR-1018 and 1018-K6 were completely stable after 24 h storage at 4 °C, in brines from different cheesemakers as no precipitation or peptide alteration/degradation processes occurred during the incubations).

3.2.2. Folding kinetics

The peptide folding kinetics following the addition of SDS (10 mM final concentration) were studied (Fig. 2) by CD and tryptophan fluorescence, to probe the formation of secondary and tertiary structures during 24 h incubation at 25 °C. Concerning 1018-K6, a band at 215 nm in CD spectra (corresponding to the formation of β-sheet structure) appeared immediately after the SDS addition with a minimum at 222 nm (corresponding to α-helix structure) gradually shifted after about 3 h. In contrast, IDR-1018 folding kinetic was slower, revealing strong conformational fluctuation over the experimental time span (Fig. 2A). These results were further validated by analyzing the time variation of α-helix and β-sheet contents of the two peptides (Tables S4, S5) showing an incremental level of secondary structures within the first 3 h of incubation for 1018-K6, which then remained substantially stable up to 24 h (Table S4). Conversely, IDR-1018

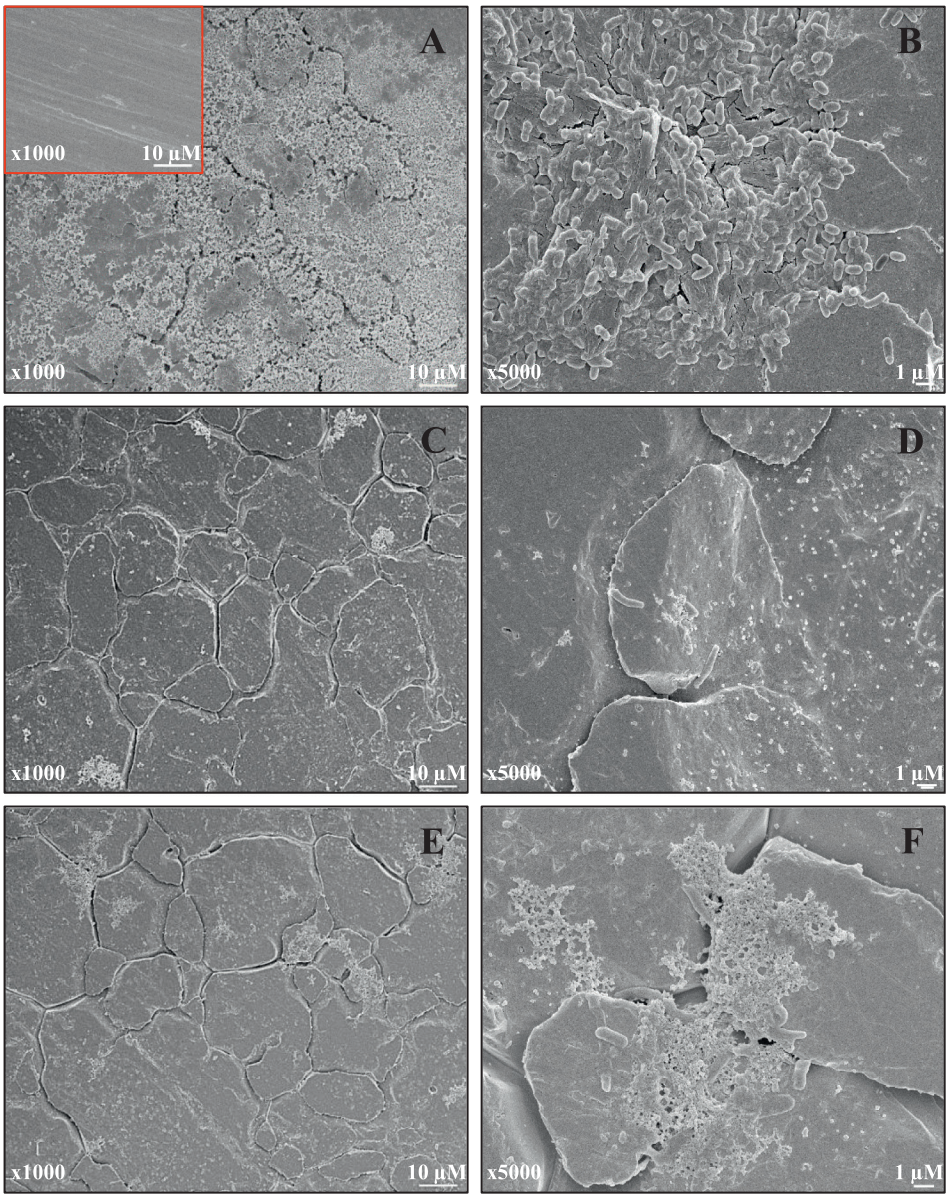

Fig. 6. SEM images of L. *monocytogenes* biofilm on stainless steel surfaces. Biofilm development observed on the steel surface, after 72 h of incubation with bacterial cultures. Surface-adhered cells were examined under a Jeol 6700 FEG–field emission SEM. Panels show representative SEM images of biofilm formation in the absence of peptides (A, B at ×1000 and ×5000 magnifications, respectively), after treatment with 50 µM of 1018-K6 (C, D at ×1000 and ×5000 magnifications, respectively) or IDR-1018 (E, F at ×1000 and ×5000 magnifications, respectively); the insert in panel A represents an image of the stainless steel surface.

displayed significant alterations of molecular folding during the whole incubation time (Table S5). Moreover, when the folding kinetics were monitored by fluorescence spectroscopy, both peptides showed a significant decrease (~20 nm) of the maximum wavelength (blue shift) immediately after SDS addition, while in the absence of SDS the two molecules appeared in unfolded states with the environments surrounding tryptophan, comparable to the free residue in solution (Fig. 3). The fluorescence spectra of folded 1018-K6 in SDS micellar solution, also revealed a large reduction in the maximal intensity (MI), compared with the quenching seen for IDR-1018. This behavior suggested that during the folding process the tryptophan residue was sequestered in the largely buried environment, resulting in much more hydrophobic in the 1018-K6 structure with respect to that of IDR-1018. Finally, the folding kinetics examined by tryptophan fluorescence were slower for both peptides compared to those observed by CD measurements, indicating an initial conformational state characterized by rearrangements of secondary structure elements of intermediates, which were faster for 1018-K6, following by the assessment of the peptide tertiary structures over 24 h (Fig. 3). Taken together, these results strongly reinforce the idea that a single amino-acid substitution, (specifically A → K) in the IDR-1018 sequence, can produce a remarkably diverse peptide conformation, which can also affect the peptide structure stability as well as its function under specific environmental conditions.

3.3. Antibacterial activity

The antimicrobial activity of 1018-IDR and 1018-K6 was tested against the Gram-positive L. *monocytogenes* and *S. aureus* and the Gram-negative *S.* Typhimurium bacteria. Since the growth of L. *monocytogenes* strains in different food product environments can remarkably modify their virulence and the pathogenicity (Hernandez-Milian and Payeras-Cifre, 2014; Jensen et al., 2016), we decided to investigate the *in vitro* antimicrobial activity of the two peptides on multiple strains of L.

monocytogenes. Specifically, we used the reference NCTC11994, and two strains selected from seafood samples, the isolates LM1 and LM2. As reported in Fig. 4, both peptides showed a strong ability to efficiently kill the reference L. *monocytogenes* strain, which was more sensitive to IDR-1018 exposure than 1018-K6, within 6 h of incubation. The peptides affected the bacterial count, already at 0.2 μM and no viable cells were detected at about 1 μM and 10 μM for IDR-1018 and 1018-K6, respectively. The dose-response inhibition curves, for the reference *Listeria* strains, allowed to determine the half-maximal effective concentrations (EC_{50}), which corresponded to 0.22 ± 0.02 μM and 0.55 ± 0.07 μM for IDR-1018 and 1018-K6, respectively (Fig. 4). Interestingly, when the two L. *monocytogenes* food-isolated strains, LM1 and LM2, were examined for susceptibility to IDR peptides, a different behavior was observed, revealing EC_{50} values for 1018-K6 treatments, two-five-fold lower than those measured using the peptide IDR-1018 (Fig. 4), with MBCs of about 10 μM and 1 μM for IDR-1018 and 1018-K6, respectively against LM1 and 20 μM and 3 μM for IDR-1018 and 1018-K6, respectively against LM2. This is notable, considering that L. *monocytogenes* strains isolated from food products or human *listeriosis* cases, often displayed strong adaptation or resistance phenomena to antibiotics and disinfectants, possibly due to the presence of mobile genetic elements carrying resistance genes or an altered permeability of the bacterial cell wall, such as structural modifications or a consequence of the action of active pumps which detoxify the cell (Charpentier and Courvalin, 1999; Knudsen et al., 2016).

Indeed, to give more consistency to the results concerning the antimicrobial activity against the foodborne pathogens, the two molecules were also tested on further three L. *monocytogenes* strains (LM3-LM5) isolated from environments of food processing industries (dairy products and canned food) (Table S1). The preliminary results confirmed an efficient bactericidal activity of 1018-K6 towards the tested strains, with MBC values < 6 μM, respect to those < 24 μM observed for IDR-1018 (data not shown). The five food-isolated strains (LM1-LM5) of L. *monocytogenes* were also characterized by PFGE revealing that four out of five are serotype 4b (LM1, LM2, LM4, LM5), while strain LM3 is serotype 1/2c (TE_ID6850). Strains TE_ID 6852 and TE_ID7850/1 were also identical based on PFGE profile (Table S1).

Conversely, when antimicrobial activities, in terms of EC_{50} values were assessed against *S. aureus* and *S.* Typhimurium (Fig. 4), a lower bactericidal efficiency was measured for both peptides in comparison with. *L. monocytogenes*, which was mainly evident in the case of 1018-K6 (Fig. 4). To test our *in silico* approach we chose, as a negative control (here named Pep-C), a previously described peptide (Falcigno et al., 2016; Palmieri et al., 2016) showing a very low Boman index (Table S2). The evaluation of the antibacterial activity of Pep-C confirmed a poor efficiency against L. *monocytogenes* and *S.* Typhimurium strains with EC_{50} values > 100 μM (data not shown). Remarkably, all the antimicrobial assays were performed by using a bacterial load of about 3.0 log CFU/ml, which represents a realistic approximation of the contamination levels that might be found in freshly prepared food products (Palmieri et al., 2016).

Further investigations are needed to better elucidate the specificity of 1018-K6 against *L monocytogenes* strains in order to identify its antimicrobial mechanism, taking into account that the components and the different structure of the bacterial membranes could greatly affect the antimicrobial activity. These results can be relevant in the context of a Risk Management Program for the development of alternative disinfection strategies to control L. *monocytogenes* contamination in the food production environments.

3.4. Antibiofilm activity

In the context of the food security, with the aim of improving the control of L. *monocytogenes* in the food industry, the antibiofilm ability of IDR-1018 and its derivative 1018-K6 was assessed by CV staining method on SS, used as food-contact surfaces in the food-processing facilities. As shown in Fig. 5, both peptides were able to inhibit biofilm growth at concentrations over 10 μM, which is higher than those able to inactivate the planktonic L. *monocytogenes*. This is not surprising, considering that generally, biofilms are much more resistant to antimicrobial agents than the planktonic counterparts. However, biofilm biomass was significantly reduced of about 70%–80%, upon peptide challenge at a concentration of 25 μM (Fig. 5). In addition, while the $MBIC_{100}$ value (minimal biofilm inhibitory concentration) evaluated for 1018-K6 was in the range 25–50 μM, the peptide IDR-1018 was not able to totally inhibit biofilm production even at 50 μM (Fig. 5), suggesting that the conformations adopted by the 1018-K6 variant could be more suitable than those of the parental compound in preventing biofilm growth of L. *monocytogenes*.

Indeed, a better killing activity of 1018-K6 than that observed for IDR-1018 was also evidenced in the bactericidal assays, specifically against *Listeria* strains isolated from foods and food-processing environments, with a significant improvement in the EC_{50} and MBC values. Finally, although the antibiofilm efficiency of both peptides appeared weaker in comparison to that reported for IDR-1018 against Gram-negative bacteria (de la Fuente-Núñez et al., 2014a, 2014b) however, as recently evidenced (Andresen et al., 2016), the peptide effects against biofilms are generally strongly dependent on the experimental approach and technical devices adopted for antibiofilm detection, which could favor inhibition of biofilms by hydrophobic cationic peptides and overestimate their real effectiveness (Andresen et al., 2016).

The antibiofilm activity of the two peptides against L. *monocytogenes* was also evaluated using scanning electron microscopy (SEM). SEM images, showing the effects of peptide treatments on biofilm formation, were developed on SS by incubating bacterial culture with two different concentrations (25 and 50 μM) of IDR-1018 and 1018-K6. Biofilms were observed using SEM at a magnification of 1000× and 5000× and five/ten microscopic random areas of the biofilm on each disk were examined. Bacterial treatments with both peptides significantly reduced the biofilm formation at 25 μM concentration (data not shown), but incubations with 50 μM of IDR-1018 (Fig. 6C, D) or 1018-K6 (Fig. 6E, F) reached the best results. Images of peptides treated samples, at 1000× magnifications (Fig. 6C, E) contained rare scattered cells than the control SS (Fig. 6A), which presented a well-defined biofilm of L. *monocytogenes*. Higher magnifications (5000×), showing a detail of biofilm formation, evidenced a well-structured biofilm in the control panel (Fig. 6B) and the almost complete absence of bacterial cells in samples incubated with the two peptides, supporting the claim of a real ability of the two molecules to inhibit L. *monocytogenes* biofilm production. However, a comparison of the images in panel D and F indicated that 1018-K6 was a more efficient inhibitor of biofilm formation than IDR-1018.

Finally, SEM pictures displayed a significant amount of extracellular debris probably derived from peptide-killed cells, showing also that biofilm cells exhibited disrupted or irregular morphologies in the treated samples.

4. Conclusion

Listeriosis is a disease most frequently induced by the exposure to contaminated food sources. Raw materials coming into the food production chain and carrying transient and persistent L. *monocytogenes* strain, represent the main cause of contamination (Jensen et al., 2016; Orsi et al., 2011). Therefore, even though most of the raw food is usually eaten after cooking, the risk of *listeriosis* should not be underestimated as the consumption of these food products is increasing worldwide. Most people are able to self-limit the *Listeriosis* disease, but individuals under immune-depressed conditions, are at higher risk for getting the disease. In addition, biofilm formation provides L. *monocytogenes* a high tolerance to antimicrobials allowing a long-term persistence of this pathogen in food-related environments, which can lead

to the transmission of resistance to the human microbiome through the ingested food. (Ayaz and Erol, 2010; Jensen et al., 2016; Knudsen et al., 2016). Therefore, this work was aimed at improving the control of L. *monocytogenes* in the food industry through the identification of a new compound, a 1018-modified peptide, named 1018-K6, having a remarkable structural stability and antibacterial activity. Specifically, 1018-K6 showed stronger efficiency than IDR-1018 in inhibiting biofilm growth and killing planktonic cells, using *Listeria* strains isolated from food-products and food-processing environments, which displayed an unusual increased susceptibility to 1018-K6 treatments. Furthermore, CD and fluorescence spectroscopy investigations on the two peptides, evidenced an enhanced propensity for helical structuring of 1018-K6 in SDS micellar solutions, which can account for the improved listericidal efficiency. Therefore, 1018-K6 represents a promising candidate for the development of alternative disinfection strategies, taking into account that the antibiofilm assays were performed on SS, largely used as contact surfaces in the food-processing facilities and that at present, there are very few studies focusing on the potential use of AMPs in the field of food sanitation and safety.

Supplementary data to this article can be found online at https://doi.org/10.1016/j.ijfoodmicro.2018.04.039.

Acknowledgments

This work was supported by: PON-RICERCA E COMPETITIVITÀ 2007–2013, MAREA (Materiali Avanzati per il comparto agroalimentare-PON03PE_00106_1); Ministero della Salute, Ricerca Corrente 2015 IZS ME 09/15 RC, una nuova classe di peptidi antimicrobici per migliorare la sicurezza degli alimenti: dal design *in silico* alla caratterizzazione strutturale e funzionale; Ministero della Salute, Ricerca Corrente 2016 IZS ME 01/16 RC, Sviluppo di metodologie innovative per ridurre il rischio di malattie trasmesse da alimenti in prodotti della filiera ittica.

The authors would like to thanks Prof. L. Nicolais and Materias srl for their support and valuable suggestions to improve the quality of the paper.

References

Abdul-Gader, A., Miles, A.J., Wallace, B.A., 2011. A reference dataset for the analyses of membrane protein secondary structures and transmembrane residues using circular dichroism spectroscopy. Bioinformatics 27, 1630–1636.

Amer, L.S., Bishop, B.M., van Hoek, M.L., 2010. Antimicrobial and antibiofilm activity of cathelicidins and short, synthetic peptides against *Francisella*. Biochem. Biophys. Res. Commun. 396, 246–251.

Andresen, L., Tenson, T., Hauryliuk, V., 2016. Cationic bactericidal peptide 1018 does not specifically target the stringent response alarmone (p)ppGpp. Sci. Rep. 6, 36549. http://dx.doi.org/10.1038/srep36549 PMCID: PMC5098146.

Ayaz, N.D., Erol, I., 2010. Relation between serotype distribution and antibiotic resistance profiles of *Listeria monocytogenes* isolated from ground Turkey. J. Food Prot. 73 (5), 967–972.

Bals, R., 2000. Epithelial antimicrobial peptides in host defense against infection. Respir. Res. 1, 141–150.

Boman, H.G., 2003. Antibacterial peptides: basic facts and emerging concepts. J. Intern. Med. 254, 197–215.

Carpentier, B., Cerf, O., 2011. Review—persistence of *Listeria monocytogenes* in food industry equipment and premises. Int. J. Food Microbiol. 145 (1), 1–8. http://dx.doi.org/10.1016/j.ijfoodmicro.2011.01.005.

Charpentier, E., Courvalin, P., 1999. Antibiotic resistance in *Listeria* spp. Antimicrob. Agents Chemother. 43 (9), 2103–2108.

de la Fuente-Núñez, C., Korolik, V., Bains, M., Nguyen, U., Breidenstein, E.B., Horsman, S., Lewenza, S., Burrows, L., Hancock, R.E.W., 2012. Inhibition of bacterial biofilm formation and swarming motility by a small synthetic cationic peptide. Antimicrob. Agents Chemother. 56, 2696–2704.

de la Fuente-Núñez, C., Reffuveille, F., Haney, E.F., Straus, S.K., Hancock, R.E.W., 2014a. Broad-spectrum anti-biofilm peptide that targets a cellular stress response. PLoS Pathog. 10 (5), e1004152. http://dx.doi.org/10.1371/journal.ppat.1004152.

de la Fuente-Núñez, C., Mansour, S.C., Wang, Z., Jiang, L., Breidenstein, E.B.M., Elliott, M., Reffuveille, F., Speert, D.P., Reckseidler-Zenteno, S.L., Shen, Y., Haapasalo, M., Hancock, R.E.W., 2014b. Anti-biofilm and immunomodulatory activities of peptides that inhibit biofilms formed by pathogens isolated from cystic fibrosis patients. Antibiotics 3 (4), 509–526. http://dx.doi.org/10.3390/antibiotics3040509.

De Smet, K., Contreras, R., 2005. Human antimicrobial peptides: defensins, cathelicidins and histatins. Biotechnol. Lett. 27, 1337–1347.

Falcigno, L., Palmieri, G., Balestrieri, M., Proroga, Y.T.R., Facchiano, A., Riccio, A., Capuano, F., Marrone, R., Campanile, G., Anastasio, A., 2016. NMR and computational data of two novel antimicrobial peptides. Data in Brief 8, 62–569.

Food and Drug Administration, Center for Food Safety and Applied Nutrition (FDA/CFSAN), 2002. Bacteriological Analytical Manual (BAM) (Chapter 11). https://www.fda.gov/Food/FoodScienceResearch/LaboratoryMethods/ucm2006948.htm.

Gilot, P., Genicot, A., Andre, P., 1996. Serotyping and esterase typing for analysis of *Listeria monocytogenes* populations recovered from foodstuffs and from human patients with listeriosis in Belgium. J. Clin. Microbiol. 34 (4), 1007–1010.

Guruprasad, K., Reddy, B.V., Pandit, M.W., 1990. Correlation between stability of a protein and its dipeptide composition: a novel approach for predicting *in vivo* stability of a protein from its primary sequence. Protein Eng. 4 (2), 155–161.

Henzler Wildman, K.A., Lee, D.K., Ramamoorthy, A., 2003. Mechanism of lipid bilayer disruption by the human antimicrobial peptide, LL-37. Biochemistry 42, 6545–6558.

Hernandez-Milian, A., Payeras-Cifre, A., 2014. What is new in listeriosis? Biotechnol. Res. Int. 358051. Epub Apr 14 2014. https://doi.org/10.1155/2014/358051.

ISO 11290-1: 1996/Amd 1, 2004. Microbiology of food and animal feeding stuffs—Horizontal method for the detection and enumeration of *Listeria monocytogenes*—Part 1: Detection method. International Standardization Organization, Geneva, Switzerland.

ISO, 11290-2: 1998/Amd 1, 2004. Microbiology of Food and Animal Feeding Stuffs—Horizontal Method for the Detection and Enumeration of *Listeria monocytogenes*—Part 2: Enumeration Method. International Standardization Organization, Geneva, Switzerland.

Jensen, A.K., Björkman, J.T., Ethelberg, S., Kiil, K., Kemp, M., Nielsen, E.M., 2016. Molecular typing and epidemiology of human Listeriosis cases, Denmark, 2002-2012. Emerg. Infect. Dis. 22 (4), 625–633. http://dx.doi.org/10.3201/eid2204.150998.

Knudsen, G.M., Fromberg, A., Ng, Y., Gram, L., 2016. Sublethal concentrations of antibiotics cause shift to anaerobic metabolism in *Listeria monocytogenes* and induce phenotypes linked to antibiotic tolerance. Front. Microbiol. 12 (7), 1091. http://dx.doi.org/10.3389/fmicb.2016.01091.

Lobley, A., Whitmore, L., Wallace, B.A., 2002. DICHROWEB: an interactive website for the analysis of protein secondary structure from circular dichroism spectra. Bioinformatics 18, 211–212.

Orsi, R.H., den Bakker, H.C., Wiedmann, M., 2011. *Listeria monocytogenes* lineages: genomics, evolution, ecology, and phenotypic characteristics. Int. J. Med. Microbiol. 301 (2), 79–96. http://dx.doi.org/10.1016/j.ijmm.2010.05.002.

Overhage, J., Campisano, A., Bains, M., Torfs, E.C., Rehm, B.H., Hancock, R.E.W., 2008. Human host defense peptide LL-37 prevents bacterial biofilm formation. Infect. Immun. 76, 4176–4182.

Palmieri, G., Balestrieri, M., Proroga, Y.T., Falcigno, L., Facchiano, A., Riccio, A., Capuano, F., Marrone, R., Neglia, G., Anastasio, A., 2016. New antimicrobial peptides against foodborne pathogens: from *in silico* design to experimental evidence. Food Chem. 211, 546–554.

Parker, W., Song, P.S., 1992. Protein structures in SDS micelle-protein complexes. Biophys. J. 61, 1435–1439.

Pena, O.M., Afacan, N., Pistolic, J., Chen, C., Madera, L., Falsafi, R., Fjell, C.D., Hancock, R.E.W., 2013. Synthetic cationic peptide IDR-1018 modulates human macrophage differentiation. PLoS One 8, e52449.

Pompilio, A., Scocchi, M., Pomponio, S., Guida, F., di Primio, A., Fiscarelli, E., Gennaro, R., Di Bonaventura, G., 2011. Antibacterial and anti-biofilm effects of cathelicidin peptides against pathogens isolated from cystic fibrosis patients. Peptides 32, 1807–1814.

PulseNet-International, 2013. Standard operating procedure for pulsenet PFGE of *Listeria monocytogenes*. http://www.cdc.gov/pulsenet/PDF/listeria-pfge-protocol-508c.pdf.

Radzicka, A., Wolfenden, R., 1988. Comparing the polarities of the amino-acids: side-chain distribution coefficients between the vapor phase, cyclohexane, 1-octanol, and neutral aqueous solution. Biochemistry 27 (5), 1664–1670.

Reffuveille, F., de la Fuente-Núñez, C., Mansour, S., Hancock, R.E.W., 2014. A broad spectrum anti-biofilm peptide enhances antibiotic action against bacterial biofilms. Antimicrob. Agents Chemother. 58, 5363–5371. http://dx.doi.org/10.1128/AAC.03163-14.

Sreerama, N., Woody, R.W., 2000. Estimation of protein secondary structure from CD spectra: comparison of CONTIN, SELCON and CDSSTR methods with an expanded reference set. Anal. Biochem. 287, 252–260.

Stewart, P.S., 2015. Antimicrobial Tolerance in Biofilms. Microbiol. Spectr. 3 (3). http://dx.doi.org/10.1128/microbiolspec.

Van Stokkum, I.H.M., Spoelder, H.J.W., Bloemendal, M., Van Grondelle, R., Groen, F.C.A., 1990. Estimation of protein secondary structure and error analysis from CD spectra. Anal. Biochem. 191, 110–118.

Wang, G., Li, X., Wang, Z., 2016. APD3: the antimicrobial peptide database as a tool for research and education. Nucleic Acids Res. 44, D1087–D1093.

Whitmore, L., Wallace, B.A., 2004. DICHROWEB: an online server for protein secondary structure analyses from circular dichroism spectroscopic data. Nucleic Acids Res. 32, 668–673.

Whitmore, L., Wallace, B.A., 2008. Protein secondary structure analyses from circular dichroism spectroscopy: methods and reference databases. Biopolymers 89, 392–400.

Wieczorek, M., Jenssen, H., Kindrachuk, J., Scott, W.R.P., Elliott, M., Hilpert, K., Cheng, J.T.J., Hancock, R.E.W., Straus, S.K., 2010. Structural studies of a peptide with immune modulating and direct antimicrobial activity. Chem. Biol. 17, 970–980.

Zelezetsky, I., Tossi, A., 2006. Alpha-helical antimicrobial peptides—using a sequence template to guide structure-activity relationship studies. Biochim. Biophys. Acta 1758, 1436–1449.